J|A|C|S
ARTICLES
Published on Web 01/31/2006

Solution State Structure Determination of Silicate Oligomers by ^{29}Si NMR Spectroscopy and Molecular Modeling

Herman Cho,*,† Andrew R. Felmy,† Raluca Craciun,‡ J. Patrick Keenum,‡ Neil Shah,‡ and David A. Dixon‡

Contribution from the Pacific Northwest National Laboratory, P.O. Box 999, Richland, Washington 99352, and Department of Chemistry, Box 870336, University of Alabama, Tuscaloosa, Alabama 35487-0336

Received August 28, 2005; E-mail: hm.cho@pnl.gov

Abstract: Evidence for nine new solution state silicate oligomers has been discovered by ^{29}Si NMR homonuclear correlation experiments of ^{29}Si-enriched samples. In addition to enhancing signal sensitivity, the isotopic enrichment increases the probability of the ^{29}Si−^{29}Si two-bond scalar couplings that are necessary for the observation of internuclear correlations in 2-D experiments. The proposed assignments are validated by comparisons of experimental and simulated cross-peaks obtained with high digital resolution. The internuclear connectivity indicated by the NMR data suggests that several of these oligomers can have multiple stereoisomers, including conformers and/or diastereomers. The stabilities of these oligomers and their possible stereoisomers have been investigated by electronic structure calculations.

1. Introduction

Silicates dissolved in water have long been a subject of inquiry because of their geochemical and industrial significance.[1] While few naturally occurring biological processes involving silicates have been found,[1,2] solution state silicates have attracted attention in biochemical contexts because of recent discoveries of interesting reactions with proteins[3] and carbohydrates.[4] Other current research on the aqueous solution behavior of silicates has been stimulated by the proposal that such species could promote the solubility of radioisotopes in the environment.[5]

Although the dominant silicate species in solution is usually the silicic acid monomer (designated Q^0 in the nomenclature of Engelhardt and co-workers[6,7]), many important processes and reactions, including gel and colloid formation[1] and solubilization of toxic metals,[5,8,9] are associated with larger oligomers that become populated only at high concentrations. It is generally accepted that 16 distinct oligomers beyond the dimer have been conclusively identified in aqueous solutions to date, with the largest of these containing eight silicon atoms (Figure 1).[10−12]

The most valuable source of information for the identification of oligomers beyond the monomer and dimer has been solution state ^{29}Si NMR measurements.[6,7,15−27] However, despite past

† Pacific Northwest National Laboratory.
‡ University of Alabama.

(1) Iler, R. K. *The Chemistry of Silica*; Wiley-Interscience: New York, 1979.
(2) Mohn, G. *Ann. University Sarav. Med.* **1974**, *21*, 63−136. Hunter, M. J.; Aberg, B. *Acta Pharmacol. Toxicol. Suppl. 3* **1975**, *36*, 9−16. *Silicon and Silaceous Structures in Biological Systems*; Simpson, T. L.; Volcani, B. E., Eds.; Springer: New York, 1981. Brook, M. A. *Silicon in Organic, Organometallic, and Polymer Chemistry*; Wiley: New York, 2000.
(3) Cha, J.; Shimizu, K.; Zhou, Y.; Christiansen, S. C.; Chmelka, B. F.; Stucky, G. D.; Morse, D. E. *Proc. Natl. Acad. Sci. U.S.A.* **1999**, *96*, 361−365. Kröger, N.; Deutzmann, R.; Sumper, M. *Science* **1999**, *286*, 1129−1132. Kröger, N.; Deutzmann, R.; Bergsdorf, C.; Sumper, M. *Proc. Natl. Acad. Sci. U.S.A.* **2000**, *97*, 14133−14138. Kröger, N.; Lorenz, S.; Brunner, E.; Sumper, M. *Science* **2002**, *298*, 584−586.
(4) Kinrade, S. D.; Del Nin, J. W.; Schach, A. S.; Sloan, T. A.; Wilson, K. L.; Knight, C. T. G. *Science* **1999**, *285*, 1542−1545. Benner, K.; Klüfers, P.; Schuhmacher, J. *Z. Inorg. Allg. Chem.* **1999**, *625*, 541−543. Benner, K.; Klüfers, P.; Vogt, M. *Angew. Chem., Int. Ed.* **2003**, *42*, 1058−1062. Kinrade, S. D.; Hamilton, R. J.; Schach, A. S.; Knight, C. T. G. *J. Chem. Soc., Dalton Trans.* **2001**, 961−963. Kinrade, S. D.; Deguns, E. W.; Gillson, A.-M. E.; Knight, C. T. G. *J. Chem. Soc., Dalton Trans.* **2003**, 3713−3716. Lambert, J. B.; Lu, G.; Singer, S. R.; Kolb, V. M. *J. Am. Chem. Soc.* **2004**, *126*, 9611−9625.
(5) Porter, R. A.; Weber, W. J. *J. Inorg. Nucl. Chem.* **1971**, *33*, 2443. Satoh, I.; Choppin, G. R. *Radiochim. Acta* **1992**, *56*, 85−87. Moll, H.; Geipel, G.; Brendler, V.; Bernhard, G.; Nitsche, H. *J. Alloys Compounds* **1998**, *271−273*, 765−768. Wadsak, W.; Hrnecek, E.; Irlweck, K. *Radiochim. Acta* **2000**, *88*, 61−64. Wang, Z.; Felmy, A. R.; Xia, Y.; Qafoku, O.; Yantasee, W.; Cho, H. M. *Radiochim. Acta* **2005**, *93*, 741−748.
(6) Engelhardt, G.; Jancke, H.; Hoebbel, D.; Wieker, W. *Z. Chem.* **1974**, *14*, 109−110.
(7) Engelhardt, G.; Zeigan, D.; Jancke, H.; Hoebbel, D.; Wieker, W. *Z. Anorg. Allg. Chem.* **1975**, *418*, 17−28.
(8) Taylor, P. D.; Jugdaohsingh, R.; Powell, J. J. *J. Am. Chem. Soc.* **1997**, *119*, 8852−8856.
(9) Swaddle, T. W. *Coord. Chem. Rev.* **2001**, *219−221*, 665−686.
(10) Marsmann, H. C. In *Encyclopedia of Nuclear Magnetic Resonance*; Grant, D. M., Harris, R. K., Eds.; Wiley: Chichester, 1996; pp 4386-4398.
(11) Sjöberg, S. *J. Non-Cryst. Solids* **1996**, *196*, 51−57.
(12) We have excluded other proposed oligomers[9,11,13,14] because they require special conditions for their formation or the spectroscopic evidence for their existence is weaker.
(13) Kinrade, S. D.; Swaddle, T. W. *Inorg. Chem.* **1988**, *27*, 4253−4259.
(14) Harris, R. K.; Bahlmann, E. K. F.; Metcalfe, K.; Smith, E. G. *Magn. Reson. Chem.* **1993**, *31*, 743−747.
(15) Harris, R. K.; Knight, C. T. G. *J. Chem. Soc., Faraday Trans. 2* **1983**, *79*, 1539−1561.
(16) Marsmann, H. C. *Z. Naturforsch.* **1974**, *29B*, 495−499.
(17) Hoebbel, D.; Garzo, G.; Engelhardt, G.; Jancke, H.; Francke, P.; Wieker, W. *Z. Anorg. Allg. Chem.* **1976**, *424*, 115−127.
(18) Engelhardt, G.; Altenburg, W.; Hoebbel, D.; Wieker, W. *Z. Anorg. Allg. Chem.* **1977**, *428*, 43−52.
(19) Engelhardt, G.; Altenburg, W.; Hoebbel, D.; Wieker, W. *Z. Anorg. Allg. Chem.* **1977**, *437*, 249−252.
(20) Harris, R. K.; Newman, R. H. *J. Chem. Soc., Faraday Trans. 2* **1977**, *73*, 1204−1215.
(21) Hoebbel, D.; Garzo, G.; Engelhardt, G.; Ebert, R.; Lippmaa, E.; Alla, M. *Z. Anorg. Allg. Chem.* **1980**, *465*, 15−33.
(22) Harris, R. K.; Jones, J.; Knight, C. T. G.; Pawson, D. *J. Mol. Struct.* **1980**, *69*, 95−103.
(23) Marsmann, H. C. *NMR: Basic Princ. Prog.* **1981**, *17*, 65.
(24) Harris, R. K.; Knight, C. T. G.; Hull, W. E. *J. Am. Chem. Soc.* **1981**, *103*, 1577−1578.

10.1021/ja0559202 CCC: $33.50

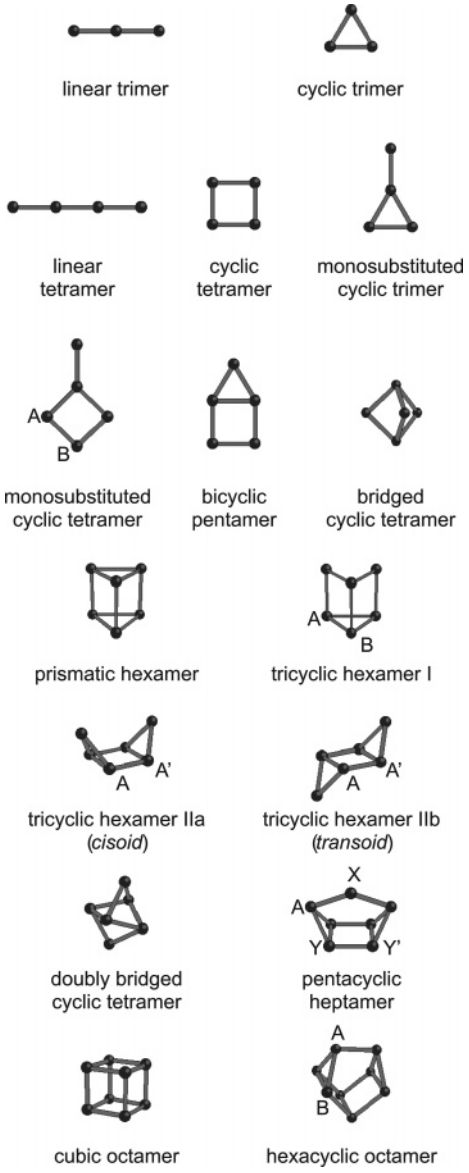

Figure 1. Solution state silicate oligomers identified in past work, excluding the monomer and dimer. By convention, balls and sticks represent silicon atoms and oxygen bridges between silicon atoms, respectively, with nonbridging oxygens omitted.

success in discovering the highest-concentration oligomers, there are numerous features in the ^{29}Si NMR spectra of silicate solutions that cannot be assigned to any of the 18 known species, as exemplified by Figure 2. Seventy-six resolved lines can be counted in this spectrum, although others have undoubtedly been missed due to spectral overlap or weak intensity. The 18 known oligomers account for only 38 of the lines and less than 87% of the total integrated signal intensity. High-resolution spectra of comparable complexity have been observed for concentrated alkali silicate solutions in past experiments.[22,26]

We describe progress in interpreting and assigning the ^{29}Si NMR spectra of aqueous silicate solutions. We propose several new oligomer structures based on an analysis of 2-D homonuclear correlation NMR spectra and electronic structure including chemical shift calculations. Silicon-29 COSY spectra of isotopically enriched silicate solutions have been previously presented by Harris et al.[28] and Knight et al.[29] These workers used the 2-D spectra to establish spectral correlations, but other useful insights available from the phases and multiplet structures of cross-peaks[30] were not discussed by them. Furthermore, previous 2-D data have been collected without multiple-quantum filtration; we have found a double-quantum filter (DQF) to be essential for suppressing the intense dispersive diagonal peaks of singlet lines, which obscure several cross-peaks and autocorrelation multiplets near the diagonal in the nonfiltered experiment.

Two samples were prepared for this study, one with ^{29}Si enrichment, and a nonenriched counterpart of otherwise identical composition. Homonuclear correlation experiments are impractical with the latter sample since they depend on the creation of multiple-quantum coherences via spin−spin interactions, which are rare in a molecule containing natural abundance levels of ^{29}Si. Because few ^{29}Si atoms are in coupled clusters in the natural abundance sample, however, the resonances in its 1-D ^{29}Si spectrum appear as singlets, which are more accurately located and integrated than the complex and overlapped multiplets of the enriched sample. Despite inferior signal intensity and an absence of spin−spin couplings, the 1-D spectrum of the natural abundance sample is thus an informative complement to the data of the enriched solution.

Candidate structures have been generated for this study taking into consideration the potential for conformational and configurational isomerism in certain oligomers. Except for the tricyclic hexamer,[15,17] the suggestion that silicate oligomers can have different isomeric forms with distinguishable NMR spectra has been absent in previous work. In the case of configurational isomers, the traditional "ball-and-stick"[10,11] method of drawing silicate oligomers can portray a deceptively simple picture of a molecule's structure by concealing the multiplicity of diastereomers and conformers that satisfy a presumptive bonding network.

The possibility of configurational isomerism follows directly from the potential chirality of Q^3 and Q^4 (but not Q^0, Q^1, or Q^2) sites. Whereas a diastereomer could represent a topological possibility for a given molecule, further evaluation is usually required to decide if a structure is physically realizable. To resolve these questions, we have used electronic structure methods at the density functional theory level to calculate the structures and relative energies of several oligomers and potential isomers. These results show that indeed there are instances where NMR signals can be explained by molecules with multiple energetically accessible diastereomers and conformers.

2. Experimental Methods

Preparation of Sodium Silicate Solutions. The entire process of preparing the NMR samples, including the filling and sealing of the NMR tubes, was performed in a controlled nitrogen atmosphere chamber (Innovative Technology) to prevent exposure of the liquids

(25) Harris, R. K.; Knight, C. T. G. *J. Mol. Struct.* **1982**, *78*, 273−278.
(26) Harris, R. K.; Knight, C. T. G. *J. Chem. Soc., Faraday Trans. 2* **1983**, *79*, 1525−1538.
(27) Engelhardt, G.; Michel, D. *High-Resolution Solid-State NMR of Silicates and Zeolites*; Wiley: New York, 1987.
(28) Harris, R. K.; O'Connor, M. J.; Curzon, E. H.; Howarth, O. W. *J. Magn. Reson.* **1984**, *57*, 115−122.
(29) Knight, C. T. G.; Kirkpatrick, R. J.; Oldfield, E. *J. Am. Chem. Soc.* **1986**, *108*, 30−33.
(30) Ernst, R. R.; Bodenhausen, G.; Wokaun, A. *Principles of Nuclear Magnetic Resonance in One and Two Dimensions*; Clarendon: Oxford, 1987.

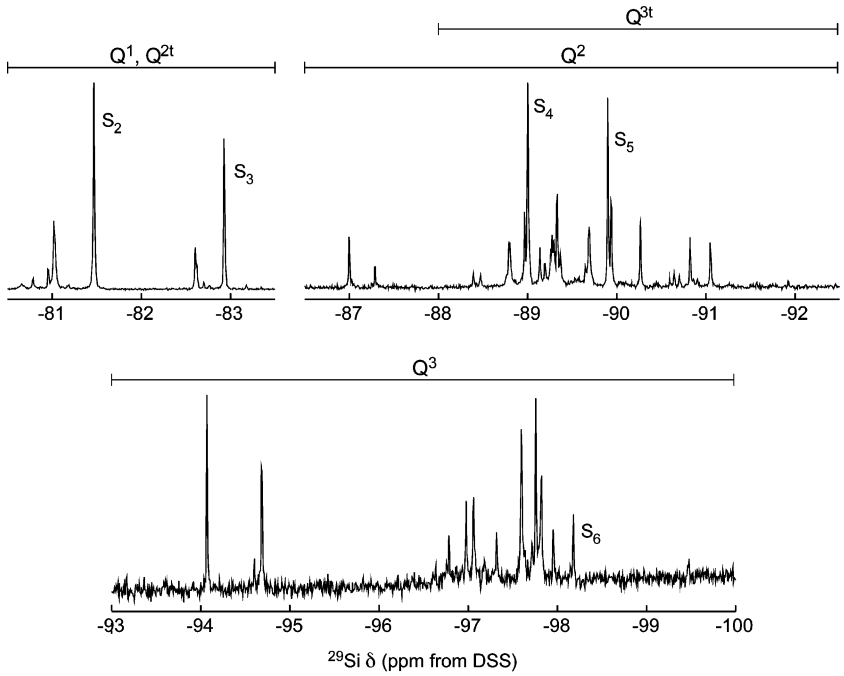

Figure 2. ^{29}Si NMR spectrum of a sodium silicate solution containing silicon with natural isotope abundances (solution **A**). The strong monomer peak at −72.77 ppm is omitted. Intensity scales are separately normalized to the highest peak in each section. Segments drawn above the spectrum denote the approximate chemical shift ranges associated with each particular Q species.[27] The "t" in some superscripts signifies a Q species that is part of a three-silicon ring. The assignment of the lines marked S_n is discussed in the Results section.

to CO_2 and O_2. Solutions were contained in polyethylene bottles at all times prior to the filling of the NMR tubes.

Deionized water and 99.99% ^{2}H-enriched water (Cambridge Isotopes Laboratory) were combined (80%/20% v/v) and boiled, and the ^{29}Si chemical shift reference compound, 3-(trimethylsilyl)-1-propane sulfonic acid (DSS), was added to the mixture to a concentration of 25 mM. Sodium hydroxide pellets (Aldrich) were added to a portion of this stock solution (**I**) to make a 2 m NaOH solution (**II**). Two identical solutions were made by pipetting 0.30 mL of **II** into 2.70 mL of **I**. To one of these solutions was added 54.9 mg of amorphous silica (solution **A**) and to the other was added an equal mass of 95% ^{29}Si-enriched silica obtained from the U.S. Department of Energy's Isotope Facility at the Oak Ridge National Laboratory (solution **B**). Both solutions were allowed to equilibrate with stirring and low heat ($T \approx 40$ °C) for 4 weeks before transferring to the NMR tubes. Silicon-29 NMR spectra recorded intermittently in the six months after the samples were created showed no visible changes.

NMR Spectroscopy. Silicon-29 NMR data were collected at 99.304 MHz on a Chemagnetics Infinity spectrometer with a 10 mm broad band Nalorac probe. The magnetic field was locked on the deuterium signal from the ^{2}H-enriched solvent. The carrier frequency was set to −85 ppm for all experiments. The typical 90° pulse time was 18 μs ($B_1 \approx 13.9$ kHz, or 140 ppm). Despite the high salt concentration of the solutions, nutation experiments we have performed indicate that undesirable sample conductivity effects were minor.

To reduce ^{29}Si background signals, NMR tubes with a bottom section made of alumina (Shigemi) were used to contain the samples. The temperature of the sample was held at 15 ± 0.2 °C by flowing thermally regulated dry nitrogen gas around the NMR tube.

One-dimensional experiments were performed with proton decoupling to facilitate accurate referencing of the chemical shift scale to the DSS ^{29}Si line. Whereas decoupling narrowed the DSS multiplet to a singlet with a line width of ≤1 Hz, it had no effect on the widths or positions of silicate resonances, in agreement with previous observations.[20]

DSS is a preferred standard for ^{1}H and ^{13}C chemical shift referencing because of the relative insensitivity of its resonances to pH, salt concentration, and temperature.[31] The silicic acid monomer peak has occasionally been chosen as an internal ^{29}Si reference for silicate chemical shifts, but we have determined DSS to be a more stable standard, especially for the alkaline, high salt conditions encountered in the study of silicate solutions. In our own ^{29}Si measurements at 15 °C, we have found that the DSS line position varies by <0.20 ppm for solvents with 0.0 M ≤ [NaOH] ≤ 2.0 M, and <0.10 ppm for 0.0 M ≤ [$NaNO_3$] ≤ 2.0 M, while for the monomer, the variation in the peak position over the same ranges is a factor of 4 or more greater.

Two-dimensional correlation spectra were acquired in the phase-sensitive mode by the method of States et al.[32] COSY experiments with double-quantum filtering were implemented according to the eight-step phase-cycling scheme of Derome and Williamson.[33]

Spin−lattice relaxation times were measured by the inversion recovery method for the ^{29}Si-enriched solution in order to determine a scan rate that would ensure quantitative integrals and minimize incomplete relaxation artifacts in 2-D experiments. The values for T_1 found in this way, most less than 15 s with several up to 20 s, were consistent with previous measurements.[10]

3. Computational Methods

NMR Spectral Simulations. Simulated 1- and 2-D oligomer time domain data sets were computed by numerical integration of the equations of motion of the ^{29}Si spin system's density matrix and then Fourier transformed to obtain the spectra. The internal Hamiltonian was assumed to consist only of isotropic chemical shifts and scalar homonuclear couplings between ^{29}Si atoms separated by only a single bridging oxygen. The C^{++} programs written for these calculations incorporate objects from the mathematical shell of the GAMMA NMR software environment.[34] The simulated COSY time domain data were

(31) Wishart, D. S.; Bigam, C. G.; Yao, J.; Abildgaard, F.; Dyson, H. J.; Oldfield, E.; Markley, J. L.; Sykes, B. D. *J. Biomolecular NMR* **1995**, *6*, 135−140.
(32) States, D. J.; Haberkorn, R. A.; Ruben, D. J. *J. Magn. Reson.* **1982**, *48*, 286−292.
(33) Derome, A. E.; Williamson, M. P. *J. Magn. Reson.* **1990**, *88*, 177−185.
(34) Smith, S.; Levante, T.; Meier, B. H.; Ernst, R. R. *J. Magn. Reson. A* **1994**, *106*, 75−105.

computed and processed as prescribed by States et al.[32] for obtaining phase-sensitive spectra.

Structure and Chemical Shift Calculations. Geometries were initially optimized and frequencies calculated (to ensure minima) at the local density functional theory level with the DZVP2 polarized double-ζ basis set on Si, H, and O.[35] No symmetry constraints were placed on any of the geometry optimizations. Many structures were optimized as initial estimates often led to structures with imaginary frequencies due to torsions about the Si−OH bonds. These imaginary frequencies were removed by adjusting the torsions about the Si−OH bonds and reoptimizing. There are many possible hydrogen bonded structures for these species. The calculations at the local level were done with the potential fit of Vosko et al.[36] for the correlation functional with Slater exchange.[37] The initial calculations of NMR chemical shifts were done with the IGLO[38] and LORG[39] approaches for treating the gauge invariance issue with the presence of the magnetic field in the electronic Hamiltonian at the local DFT level with the TZVP basis set. Our definition of the chemical shift and its relation to the shielding conform to the IUPAC recommendation.[40] The calculations were done with the program DGauss on Silicon Graphics computers.[41]

The LORG and IGLO results provided an unsatisfactory fit to the experimental data, and therefore, we have also computed the chemical shifts at the GIAO level[42] with the polarized triple-ζ basis set derived from the work of the Ahlrich group[43] and used by Moravetski et al.[44] The GIAO calculations were done at the density functional theory level with the B3LYP gradient corrected exchange-correlation functional[45] using the Gaussian-03 program.[46] The chemical shift reference compound for the computed results (DSS) was the same as the one used in the experiments. The GIAO calculations with the local DFT geometries were in closer agreement with the experimental shifts. For example, the chemical shift of $Si(OH)_4$ is calculated to be −65.7 ppm with respect to TMS as compared with the experimental result of −72.0 ppm extrapolated for $Si(OH)_4$ in aqueous solution.[47]

However, as noted above, the structures had a large number of hydrogen bonds, and because the local density approximation is not as good for such systems, the geometries were reoptimized with the gradient corrected B3LYP functional and the DZVP2 basis set; frequencies were calculated to ensure that the optimized structures were minima. The chemical shifts were recalculated at the GIAO/B3LYP/TZP level using the new B3LYP geometries. Values closer to the experimental shifts were found, and for $Si(OH)_4$, the value of the ^{29}Si shift was −69.8 ppm.

Because no symmetry constraints were imposed during the geometry optimization and because of the presence of different hydrogen bond interactions, sites that could be related by symmetry, such as the three Q^{2t} atoms in the cyclic trimer, often had slightly different chemical shifts. In these cases, the shifts of potentially symmetry related atoms were averaged to produce a single value for comparison with the experimental values. The complete Cartesian coordinates, total energies, and chemical shifts for the individual Si atoms are given as Supporting Information.

The influence of the molecular charge state on calculated ^{29}Si chemical shifts has been examined by Moravetski et al.[44] for the case of the neutral (H_4SiO_4) and singly ionized ($H_3SiO_4^-$) monomers. As isolated molecules, H_4SiO_4 and $H_3SiO_4^-$ differed by 6.2 ppm in their calculated isotropic shifts, but upon inclusion of solvent molecules and addition of counterions to the anion, the difference was reduced to as little as 0.1 ppm for some models, and closer correspondence was obtained with experimental observations. Variable pH measurements have found similar small displacements of ^{29}Si chemical shifts upon deprotonation of silicate oligomers.[13] Extrapolating from these findings, we assume that isotropic chemical shifts for neutral oligomers are a good approximation of the shifts for solvated, solution-averaged charged species and report chemical shifts for neutral molecules only.

4. Results and Discussion

Homonuclear Correlation Experiments. The 1-D ^{29}Si spectra of solutions **A** and **B** are shown in sections in Figures 2−4. The two samples are nominally identical except for their ^{29}Si abundances, which are 4.7% for **A** and 95% for **B**. All of the observed resonances in the spectrum of **A** (Figure 2) are singlets, due to the low probability that adjacent silicon atoms in a silicate network will both be of the ^{29}Si isotope. For ^{29}Si atoms at Q^1, Q^2, and Q^3 sites, the probabilities that at least one of the nearest neighbor silicon atoms is also ^{29}Si are 4.7, 9.2, and 13.4%, respectively.

Most of the resonances in Figure 2 have become multiplets in the spectrum of **B** because of the increased probability of $^{29}Si-^{29}Si$ scalar couplings between adjacent silicon sites. The exceptions are the six singlets labeled S_n, which we have identified based on previous assignments (Table 1).

At the 95% ^{29}Si enrichment level of **B**, a ^{29}Si atom at a Q^2 site has a 9.5% probability of having one ^{28}Si atom among its two silicon nearest neighbors, and a Q^3 site has a 13.5% probability of having one ^{28}Si atom among its three silicon nearest neighbors. The consequence of this distribution of finite isotopomer probabilities is displayed by the 1-D A_3X_2 spectrum of the bridged cyclic tetramer (Figure 3d), as noted by Harris et al.[26] Both the A and X spin multiplets are superpositions of resonances from isotopomers with different numbers of ^{28}Si atoms coupled to the observed spin. Besides complicating the multiplet patterns in the 1-D spectra, the mix of isotopomers also slightly distorts the classical A_3X_2 antiphase cross-peak pattern in the COSY spectrum. In general, the 1- and 2-D spectra of the enriched sample are to be interpreted as superpositions of signals from multiple isotopomers.

Sections of the COSY and DQF−COSY spectra of solution **B** are presented in Figures 3 and 4, respectively. Because of the need for long acquisition delays, the number of points collected in the indirectly detected dimension is only half the number in the directly detected dimension. The difference in spectral resolution is evident in the asymmetry across the diagonal in Figure 4, and in our analysis of cross-peak patterns, we have considered features mainly in the f_2 dimension.

The cross-peaks found in the COSY and DQF−COSY spectra are cataloged in Tables 2 and 3. Since there are slight variations in the chemical shifts of silicate sites from sample to sample, 1- and 2-D peaks were related to known oligomers by also considering the peak intensity, the multiplet structure, and the relative ordering of the peaks in the spectrum. Every cross-

(35) Godbout, N.; Salahub, D. R.; Andzelm, J.; Wimmer, E. *Can. J. Chem.* **1992**, *70*, 560−571.
(36) Vosko, S. J.; Wilk, L.; Nusair, W. *Can. J. Phys.* **1980**, *58*, 1200−1211.
(37) Slater, J. C. *Quantum Theory of Atomic Structure, Vol. 2*; McGraw-Hill: New York, 1960.
(38) Schindler, M.; Kutzelnigg, W. *J. Chem. Phys.* **1982**, *76*, 1919−1933.
(39) Hansen, A. E.; Bouman, T. D. *J. Chem. Phys.* **1985**, *82*, 5035−5047.
(40) Harris, R. K.; Becker, E. D.; Cabral de Menezes, S. M.; Goodfellow, R.; Granger, P. *Pure Appl. Chem.* **2001**, *73*, 1795−1818.
(41) Andzelm, J. W.; Wimmer, E. *J. Chem. Phys.* **1992**, *96*, 1280−1303.
(42) Wolinski, K.; Hinton, J. F.; Pulay, P. *J. Am. Chem. Soc.* **1990**, *112*, 8251−8260.
(43) Schafer, A.; Horn, H.; Ahlrichs, R. *J. Chem. Phys.* **1992**, *97*, 2571−2577.
(44) Moravetski, V.; Hill, J.-R.; Eichler, U.; Cheetham, A. K.; Sauer, J. *J. Am. Chem. Soc.* **1996**, *118*, 13015−13020.
(45) Becke, A. D. *J. Chem. Phys.* **1993**, *98*, 1372−1377. Becke, A. D. *J. Chem. Phys.* **1993**, *98*, 5648−5652. Lee, C.; Yang, W.; Parr, R. G. *Phys. Rev. B* **1988**, *37*, 785−789.
(46) Gaussian 03, Revision B.05; Frisch, M. J. et al. Gaussian, Inc.: Wallingford CT, 2004.
(47) Unger, B.; Jancke, H.; Hähnert, M.; Stade, H. *J. Sol-Gel Sci. Technol.* **1994**, *2*, 51.

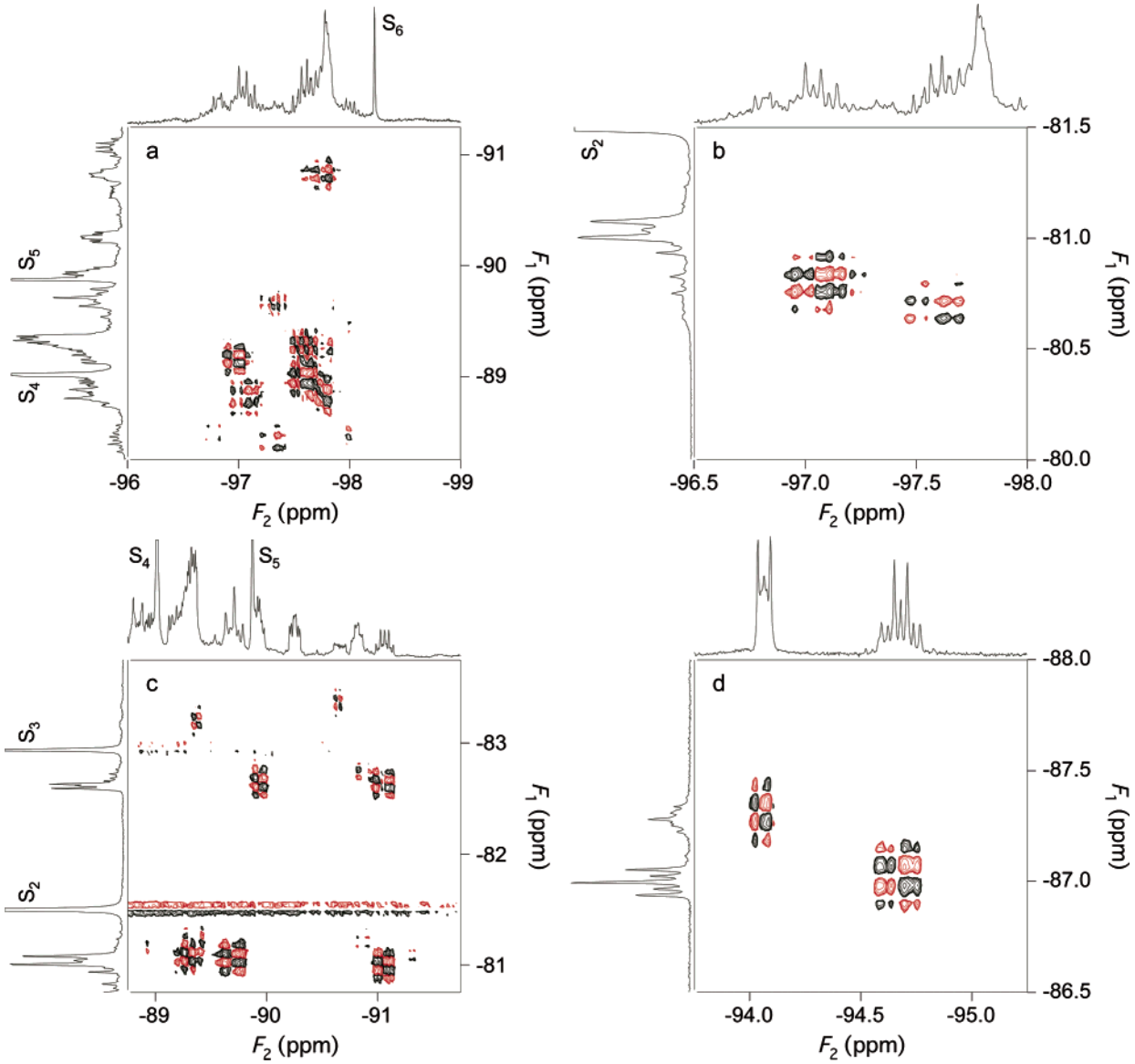

Figure 3. Various ^{29}Si COSY cross-peak regions of solution **B**, plotted with the 1-D spectra of the corresponding F_1 and F_2 spectral ranges. Intense singlet lines (designated S_n) have been truncated in the 1-D spectra. A $\pi/2$ mixing pulse was used.

peak expected for the 16 oligomers in Figure 1 were found in either or both the COSY and DQF−COSY spectra.

Cross-peaks that could not be assigned to the oligomers in Figure 1 are collected in Table 3. Cross-peaks that appear to be associated with the same oligomer because of their alignment, intensities, and similar patterns have been grouped.

Comparison of Experimental and Simulated COSY Spectra. With few exceptions, the unassigned peaks in the spectra of ^{29}Si-enriched silicate solutions lie in bands where severe overlap of resonances complicates the separation of individual multiplets from 1-D spectra. Therefore, we have relied almost entirely on analyses of 2-D spectra, which provide a much clearer picture of the multiplet structures and internuclear connectivities.

This approach was tested by comparing experimental and simulated COSY spectra for several previously identified oligomers. The inputs for these calculations were the chemical shifts determined from our own spectra, listed in Table 2, and scalar couplings obtained earlier by Harris and Knight.[15,26] In every case, the simulated COSY cross-peaks closely matched the experimental result and, thus, support the findings of Harris and Knight.

The pentacyclic heptamer, as a large spin network containing strong couplings, serves as an illustrative benchmark of this approach. Although this oligomer should have three ^{29}Si resonances, Harris and Knight were able to locate only the A and Y spin resonances and inferred the existence of an X spin from selective homonuclear decoupling experiments.[15] The COSY spectrum in Figure 5 reveals the reasons for their difficulty in finding the X spin resonance by 1-D methods. The X spin resonance is separated by just 0.26 ppm (approximately 26 Hz at 99.304 MHz) from the Y resonance and thus could easily be overlooked by techniques that depend on selective irradiation, such as 1-D homonuclear decoupling experiments. In addition, the X signal is the weakest of the three resonances and is obscured in one dimension by nearby peaks from more concentrated species, including the prismatic hexamer, hexacyclic octamer, and tricyclic hexamer IIb.

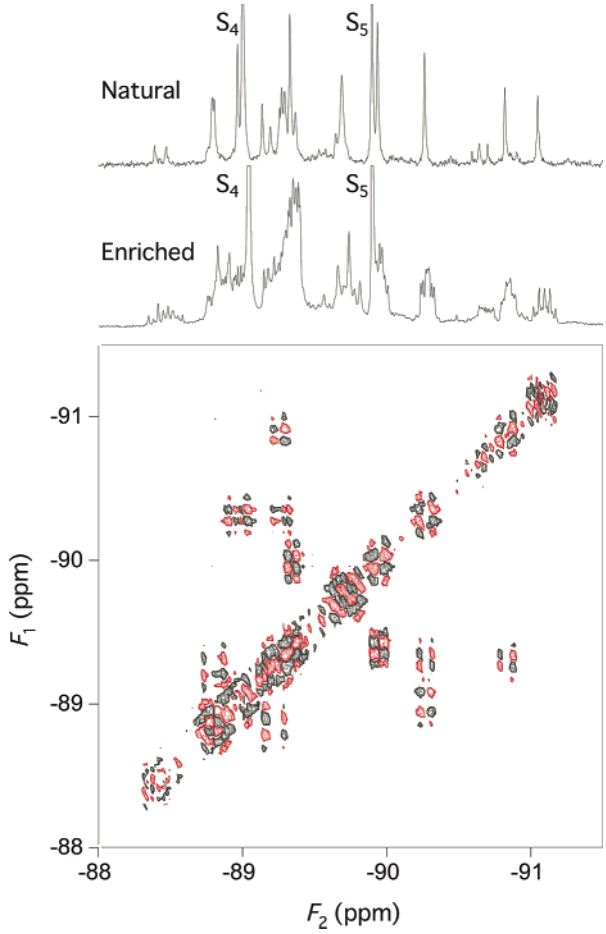

Figure 4. Diagonal region of a ^{29}Si DQF−COSY spectrum of solution **B** in a spectral range containing resonances from Q^2 and Q^{3t} sites. The 1-D spectra of solutions made with natural abundance (solution **A**) and ^{29}Si-enriched (solution **B**) silica are shown above the 2-D spectrum.

Table 1: Singlet Resonances in ^{29}Si Spectra of Concentrated Silicate Solutions

Peak ID	Chemical shift (ppm)[a]	Integrated intensity[a]	Assignment
S_1	−72.77	1.000	monomer (Q^0)
S_2	−81.47	0.440	dimer (Q^1)
S_3	−82.93	0.264	cyclic trimer (Q^{2t})
S_4	−89.00	0.161	cyclic tetramer (Q^2)
S_5	−89.90	0.109	prismatic hexamer (Q^{3t})
S_6	−98.18	0.013	cubic octamer (Q^3)

[a] From solution **A** measurements.

Despite the low concentration of the pentacyclic heptamer, which we estimate to be less than 0.5% of the silicic acid monomer, its experimental COSY cross-peaks are readily found and confirmed as being a good match of the simulated cross-peaks. The asymmetry of the X and Y resonances, which is the result of strong couplings in the spin network, is also reflected in both the simulated and experimental cross-peaks and demonstrates the sensitivity of this approach to subtle spectral features.

Strong and intermediate couplings are a common feature of silicate oligomers, besides the pentacyclic hexamer, and significantly complicate the interpretation of 1-D spectra. Even when such couplings are present, however, Figure 5 illustrates that the correlation spectra often display a simpler first order appearance, allowing the *J* value of an active coupling to be read directly from the cross-peak splittings.

Table 2: COSY and DQF−COSY Crosspeak Assignment to Known Oligomers. for Labeling of Silicon Sites, See Figure 1

Oligomer	Cross-peaks center (ppm)	Assignment
linear trimer	(−81.05, −89.69)	(Q^1, Q^2)
linear tetramer	(−81.06, −89.31)	(Q^1, Q^2)
monosubstituted cyclic trimer	(−80.98, −91.05)	(Q^1, Q^{3t})
	(−82.61, −91.05)	(Q^{2t}, Q^{3t})
monosubstituted cyclic tetramer	(−80.80, −97.08)	(Q^1, Q^3)
	(−88.80, −89.23)[a]	(Q^2(A), Q^2(B))
	(−88.80, −97.08)	(Q^2(A), Q^3)
bicyclic pentamer	(−82.63, −89.94)	(Q^{2t}, Q^{3t})
	(−89.36, −89.94)[a]	(Q^2, Q^{3t})
bridged cyclic tetramer	(−87.00, −94.68)	(Q^2, Q^3)
tricyclic hexamer I	(−88.98, −97.60)	(Q^2, Q^3)
	(−88.98, −90.28)[a]	(Q^2, Q^{3t}(A))
	(−89.28, −97.60)	(Q^{3t}(B), Q^3)
	(−89.28, −90.28)[a]	(Q^{3t}(B), Q^{3t}(A))
tricyclic hexamer IIa (*cisoid*)	(−83.19, −89.38)	(Q^{2t}, Q^{3t})
tricyclic hexamer IIb (*transoid*)	(−83.36, −90.64)	(Q^{2t}, Q^{3t})
doubly bridged cyclic tetramer	(−87.30, −94.08)	(Q^2, Q^3)
pentacyclic heptamer	(−90.43, −91.91)	(Q^2(X), Q^{3t}(A))
	(−90.69, −91.91)	(Q^{3t}(Y), Q^{3t}(A))
hexacyclic octamer	(−90.61, −93.19)	(Q^{3t}(B), Q^{3t}(A))
	(−90.61, −99.46)	(Q^{3t}(B), Q^3)

[a] From DQF−COSY spectrum.

Table 3: COSY and DQF−COSY Resonances Not Assigned to Known Oligomers

Oligomer ID	Cross-peaks center (ppm)
1	(−81.21, −90.88)
2	(−80.69, −97.58)
3	(−81.18, −89.35)
4	(−82.71, −90.88)
5	(−89.16, −96.97)
6	(−89.30, −97.81)
7	(−88.81, −89.27)[a,b]
	(−88.81, −97.76)
	(−89.27, −90.85)[a]
	(−90.85, −97.76)
8	(−88.41, −97.31)
	(−89.66, −97.31))
9	(−88.50, −96.80)
	(−89.36, −96.80)

[a] From DQF−COSY spectrum. [b] Uncertain due to overlap with cross-peak from monosubstituted cyclic tetramer.

Structure Determination. The number of theoretically possible oligomer structures rapidly grows with increasing silicon number, N_{Si}, though many can be rejected immediately. For example, the range of candidates is considerably narrowed by excluding structures with Q^4 sites, which are generally not observed under the conditions considered here.[14,24,26] In this Article, we furthermore assume that the coordination of silicon in our samples is exclusively tetracoordinate.

Experimental and theoretical studies[1,48,49] have established that solid silica, when hydrolyzed, enters the solution state as the monomer. Silicate oligomers thus form via the combination of smaller fragments in solution, with populations of higher order oligomers reaching detectable levels only when total silicon concentrations exceed certain thresholds.[50] Consistent with this, a survey of past quantitative studies reveals that the relative population of individual species is a steeply declining

(48) Fleming, B. A. *J. Colloid Interface Sci.* **1986**, *110*, 40−64.
(49) Xiao, Y.; Lasaga, A. C. *Geochim. Cosmochim. Acta* **1994**, *58*, 5379−5400.
(50) Sjöberg, S.; Öhman, L.; Ingri, N. *Acta Chem. Scand. A* **1985**, *39*, 93−107. Svensson, I. L.; Sjöberg, S.; Öhman, L. *J. Chem. Soc., Faraday Trans. 1* **1986**, *82*, 3635−3646. Felmy, A. R.; Cho, H.; Rustad, J. R.; Mason, M. J. *J. Soln. Chem.* **2001**, *30*, 509−525.

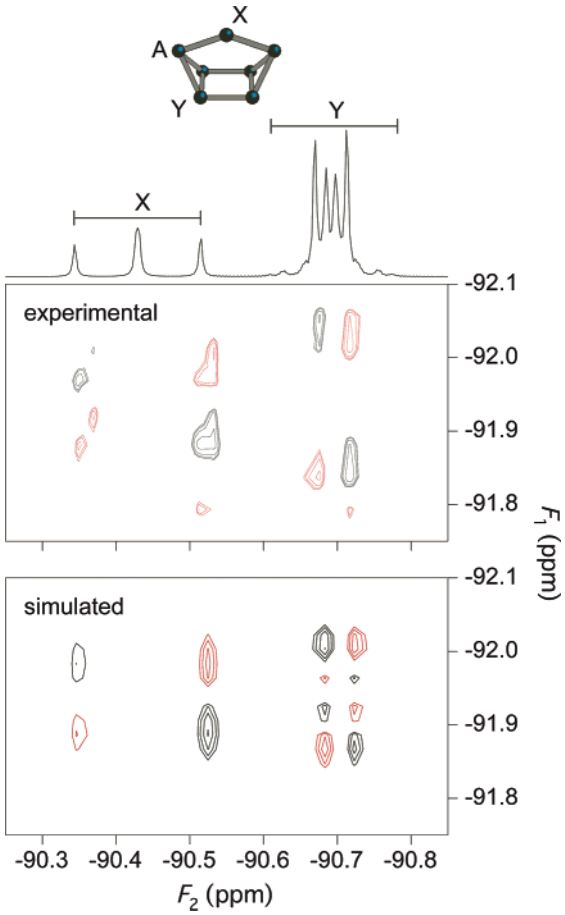

Figure 5. Experimental and simulated COSY cross-peaks of the pentacyclic heptamer. The minor central features in the simulated (Q^{3t}(A), Q^{3t}(Y)) cross-peak are below the noise level of the experimental spectrum. Extra peaks in the experimental spectrum are apodization artifacts of the t_1 dimension. The 1-D spectrum is a simulation.

function of silicon number, and the most probable oligomers are those that can be formed by bimolecular reactions of favored low order structures, such as the monomer, dimer, cyclic trimer, cyclic tetramer, etc. A logical starting strategy, therefore, is to consider candidates in order of increasing size.

Excluding structures containing Q^4 sites, every possible oligomer with $N_{Si} \leq 3$ has been experimentally discovered in previous work. For $N_{Si} = 4$, the only oligomers that have not been definitively detected in the past are the tetrahedral tetramer, the trisubstituted monomer, and the bicyclic tetramer. The structures of the latter two oligomers are characterized by a single weak scalar coupling and should exhibit only a single homonuclear correlation with easily recognized cross-peak patterns.

Since the four silicon sites in the tetrahedral tetramer are magnetically equivalent, the NMR spectrum of this oligomer should consist of a distinctive singlet in the Q^{3t} chemical shift range. Except for S_4 and S_5, which have already been assigned to other oligomers, no such signal has been definitively located either in our spectra or in previous investigations. It has been suggested that the structure may be too strained to be stable,[15] but in fact, the tetrahedral tetramer resembles adamantane, and the only strain is in the Si−O−Si bond angle, which is quite flexible, with a value of ∼115° as compared to an optimum bond angle in SiH_3OSiH_3 of ∼135°. We note that allowing hydrogen bonding from Si(OH) to another Si(OH) across an

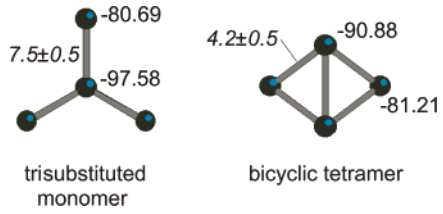

Figure 6. New silicate tetramers identified with homonuclear correlation experiments. The silicon sites are labeled with their observed chemical shifts (ppm). The scalar couplings (Hz, in italics) between silicon sites were determined directly from the cross-peak splittings; since the Q^{3t} sites of the bicyclic tetramer are magnetically equivalent, $J(Q^{3t}, Q^{3t})$ could not be measured.

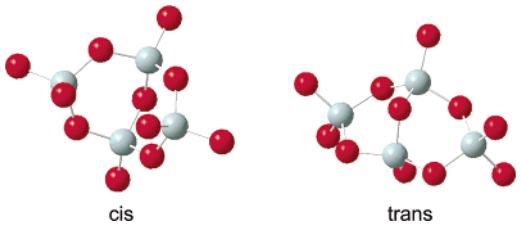

Figure 7. Energy-minimized structures of the bicyclic tetramer's diastereomers. Gray and red spheres represent Si and O atoms, respectively; hydrogen atoms on nonbridging oxygens have been omitted.

Si−O−Si bridge can reduce the bond angle to near 120°. The tetrahedral tetramer has been analyzed by Moravetski et al.,[44] who have found that this oligomer is destabilized relative to the monomer, but has a total energy that is lower than several other structures of known stability. An alternative explanation for its absence that does not rely on a stability argument is that the molecule may be difficult to form from a binary reaction of smaller oligomers. Although the tetrahedral tetramer can theoretically be created from several binary reactions, such as the combination of the cyclic trimer and the monomer, these would require the formation of three or more oxygen bridges between the reagents and, thus, would be expected to have a low probability of proceeding to completion.

The predicted COSY signature of the trisubstituted monomer is a single (Q^1, Q^3) correlation. The oligomer labeled **2** in Table 3 is the only unassigned resonance matching this description. Closer inspection of the cross-peak itself (Figure 3b) reveals that it has the appearance of a classical AX_3 pattern,[30] with a scalar coupling that can be read directly from the 2-D spectrum to be 7.5 Hz. Our conclusion therefore is that oligomer **2** is the trisubstituted monomer (Figure 6).

The bicyclic tetramer is similarly characterized by a single 2-D resonance, in this case representing a (Q^{2t}, Q^{3t}) correlation. From the positions of their correlated resonances, oligomers **1**, **3**, and **4** in Table 3 are seen to be candidates, but upon examination of the cross-peak patterns (Figure 3c), only the oligomer **1** resonance is recognizable as a classical A_2X_2 pattern, with an AX scalar coupling of 4.2 Hz. Since the bicyclic tetramer is the smallest oligomer consistent with these observations, we conclude that its identification as oligomer **1** is credible.

It is relevant to inquire why evidence for only a single bicyclic tetramer was found in the correlation spectrum. Despite the apparent simplicity of the structure in Figure 6, two diastereomers of the bicyclic tetramer can be formed by rearrangement of the coordination at the Q^{3t} sites (Figure 7). Although an energy minimum can be found for the *trans* structure, we have

calculated that it is 62.8 kcal/mol higher than the minimum of the *cis* isomer. If the populations of the two diastereomers are given by a thermal equilibrium, then only the *cis* diastereomer would be expected in detectable concentrations at room temperature. The theoretical analysis also reveals that the Q^{3t} sites of the *cis* isomer are relatively unstrained and have a chemical shift in the normal range for Q^{3t} ^{29}Si nuclei, whereas one of the Q^{3t} sites of the *trans* isomer (lower bridgehead Si in Figure 7) is quite strained with a chemical shift substantially more positive.

The concentrations of four tetramers (the linear tetramer, the cyclic tetramer, the monosubstituted cyclic trimer, and the trisubstituted monomer) can be estimated from the integrated NMR intensities of the solution **A** 1-D spectrum to be within 3−5% of the monomer concentration. The NMR intensities also indicate that no oligomer with $N_{Si} \geq 5$ has a higher concentration, and no oligomer with $N_{Si} \leq 3$ has a lower concentration than these four tetramers. The intensities of the bicyclic tetramer peaks are more difficult to determine due to spectral overlap in the 1-D spectrum; nevertheless, it is clear that this molecule is anomalous, with a concentration that is less than 20% of those of the other four tetramers. The bicyclic tetramer is unique among the tetramers in that its formation by a binary reaction of two smaller oligomers (e.g., the monomer and cyclic trimer) requires the creation of at least two Si−O−Si linkages, whereas the other tetramers can be formed via reactions in which only a single Si−O−Si linkage is created. It is therefore plausible that its probability of formation would be lower.

We have also considered assignments of cross-peak **1** to oligomers of larger size as a possible explanation of the low concentration. Since the Q^{2t} and Q^1 chemical shift ranges overlap, one alternative interpretation is to assign the −81.21 ppm line to a Q^1 site. Furthermore, it may be seen in Table 3 that oligomers **1** and **4** both have lines at −90.88 ppm, which implies that the cross-peaks could belong to the same molecule. It follows from this interpretation that the putative oligomer contains a structural unit of the form $Q^1-Q^{3t}-Q^{2t}$. Such a unit is found in both the monosubstituted and disubstituted cyclic trimers, but the former has already been located (Table 2) and thus we exclude it. We have computed cross-peak patterns for the disubstituted cyclic trimer that can be matched to the experimental patterns, but the two-bond $^{29}Si-^{29}Si$ scalar couplings we obtained are outside the credible range for these parameters, and hence this oligomer is an unlikely explanation.

Oligomer 3. The −81.18 ppm resonance of oligomer **3** lies in a range that is associated with both Q^1 and Q^{2t} sites, while the −89.35 ppm chemical shift is consistent with Q^2 and Q^{3t} sites. The ambiguity is resolved by examining the cross-peak pattern (Figure 3c), which indicates that to first order the −81.18 ppm resonance is a doublet with an 8.0 Hz splitting, and the −89.35 ppm resonance is a triplet also with 8.0 Hz splittings. The most plausible explanation is that the −81.18 and −89.35 ppm resonances correspond to Q^1 and Q^2 sites, respectively.

A 2-D cross-peak pattern that is a doublet in one dimension and a triplet in the second dimension is the signature correlation of an AX_2 spin system. The oligomer **3** cross-peak pattern is indeed almost superimposable on the COSY resonance of the linear trimer (and situated very near to it), but is considerably weaker. Since the linear trimer has already been accounted for, we turn our attention to the linear pentamer, which can be represented as an $A(BX)_2$ spin system.

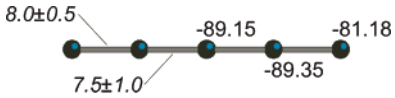

Figure 8. Proposed silicon network of oligomer **3**. The chemical shift of the middle Q^2 site and the *J* couplings are from the simulated spectrum that was the closest visual match of the experimental spectrum. The −89.15 ppm resonance was not actually observed, and therefore the parameters associated with this spin have larger uncertainties.

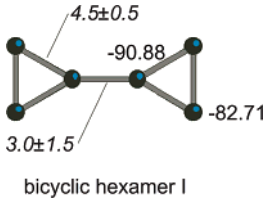

Figure 9. Proposed silicon network of oligomer **4**. The *J* values are from the simulation that was the best visual match of the experimental COSY spectrum. The *J* interaction of the magnetically equivalent Q^{2t} sites in each ring does not affect the spectrum and could not be measured.

In addition to a (B, X) correlation, the COSY spectrum of an $A(BX)_2$ spin system should contain an (A, B) correlation. No evidence of such a correlation was found in either the COSY or DQF−COSY spectrum. We hypothesize that the chemical shifts of the A and B spins, which are both Q^2 sites in a linear chain, are so close in value that the correlation peaks cannot be differentiated from autocorrelation signals. Given the numerous overlapped cross-peaks in the diagonal region of the DQF−COSY spectrum around −89.35 ppm (Figure 4), we estimate that the (A, B) correlation would not be distinguishable as an off-diagonal resonance if $|\delta(A) - \delta(B)| \leq 0.2$ ppm at 99.304 MHz. Simulations with $\delta(A) = -89.15$ ppm and a proper choice of *J*(B, X) and *J*(A, B) indicate that close correspondence with the experimental COSY spectrum can be obtained with this model. The A, B, and X multiplets deviate markedly from simple first order patterns in the 1-D spectrum because of strong coupling effects, but in the COSY spectrum, the (B, X) correlation largely retains the classical "triplet/doublet" pattern of a weakly coupled spin system. The computational results are consistent with the observed shifts.

Oligomer 4. The chemical shifts of oligomer **4**'s correlated resonances signify a single (Q^{2t}, Q^{3t}) correlation. The cross-peak pattern indicates that to first order the Q^{2t} resonance is a doublet with a 4.5 Hz splitting, while the Q^{3t} multiplet is a triplet with the same splitting (Figure 3c). The smallest spin network that is consistent with these observations is the oligomer we label as bicyclic hexamer I. This structure can be described as two cyclic trimers connected by a bridging oxygen. Simulations comparing favorably with the experimental cross-peaks can indeed be calculated with *J* values that are appropriate for the coupled Q sites (Figure 9).

The (Q^{2t}, Q^{3t}) cross-peak pattern is relatively insensitive to the strong coupling between the chemically equivalent Q^{3t} sites. Variation of *J*(Q^{3t}, Q^{3t}) was found to result mainly in subtle changes in the shapes, but not splitting, of the (Q^{2t}, Q^{3t}) cross-peak, thus the value of this parameter determined by comparison of 2-D data has an inherently large relative uncertainty.

Oligomers 5 and 6. The −96.97 ppm resonance of oligomer **5** can be confidently assigned on the basis of its chemical shift to a Q^3 site, but the −89.16 ppm resonance lies in the ranges for both Q^2 and Q^{3t} sites, and at first glance, its assignment is ambiguous. There are no simple small structures ($N_{Si} \leq 8$)

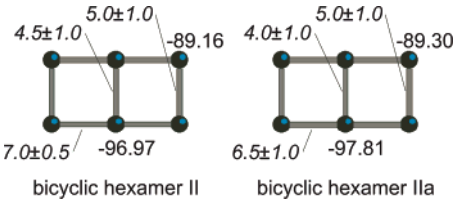

Figure 10. Proposed silicon networks of oligomers **5** and **6** with the *J* and chemical shift parameters of the simulations that were the best matches to the experimental COSY spectrum. The structures are stereoisomers of each other.

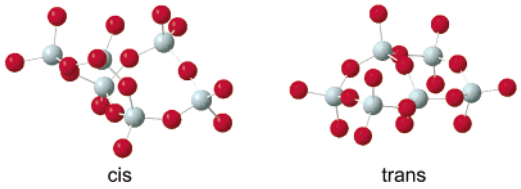

Figure 11. Energy-minimized structures of the bicyclic hexamer's diastereomers (cf. Figure 10).

consisting only of Q^3 and Q^{3t} sites, so we regard the Q^{3t} assignment as unlikely. It is possible that this oligomer has correlations that were missed in the 2-D spectra, but the large intensity of the −89.16 and −96.97 ppm peaks and their separation from other resonances in one dimension make this doubtful.

If we interpret the oligomer **5** 2-D resonance as a (Q^2, Q^3) correlation, then it follows from a first order analysis of the cross-peak pattern (Figure 3a) that the Q^2 site is actively coupled to only one Q^3 site, and the Q^3 site is actively coupled to two Q^2 sites, that is, the oligomer contains a unit of the form $Q^2-Q^3-Q^2$. The cross-peak pattern deviates slightly from a classical first order appearance, however, and thus we infer the presence of strong couplings in the structure of oligomer **5**. The smallest structure that is consistent with these observations belongs to the oligomer we label as bicyclic hexamer II. Our simulated COSY spectra confirm that the experimental cross-peak patterns can be reproduced with the structure and parameters in Figure 10.

A similar analysis holds for oligomer **6**, and therefore, we conclude that **6** is a stereoisomer of **5**. The cross-peak pattern for oligomer **6** is less clearly seen because of partial overlap with the (Q^{3t}(B), Q^3) resonance of the tricyclic hexamer I, and the uncertainties in the scalar couplings, $J(Q^2, Q^3)$, in particular, are correspondingly larger.

Electronic structure calculations verify the existence and stability of two diastereomers with similar energies, which we call the *cis* and *trans* forms (Figure 11). As for the bicyclic tetramer, the diastereomers are related by an inversion of atoms around one of the Q^3 sites. In the *cis* structure, the OH groups on the two Q^3 sites point to the same side of the molecular "plane." The *trans* linkage is formed by inverting the bonding around one of the Q^3 Si atoms, which results in one Q^3 site being strained from a tetrahedral geometry and the other unstrained.

The *trans* diastereomer has two stable conformers, with energies 6.3 and 8.1 kcal/mol above that of the *cis* form. Because of the different orientations of the OH groups, the two Q^3 sites in the *cis* structure have chemical shifts that differ by 1 ppm, whereas for the lower energy *trans* isomer, the chemical shifts of the strained Q^3 ^{29}Si site is almost 11 ppm lower than the value for the unstrained site. The shift for the unstrained site is 3 to 4 ppm below that of the Q^3 site in *cis* isomer. In both stereoisomers, we assume the Q^3 sites are rapidly interconverting so only a single ^{29}Si resonance is observed at the average line position, in accordance with the experimental finding.

Oligomer 7. From the integrated intensities of the ^{29}Si resonances, we estimate that oligomer **7** is comparable in concentration to the monosubstituted tetramer, the bridged cyclic tetramer, and tricyclic hexamer I, and at least 5 times higher in concentration than the pentacyclic heptamer. Since every oligomer with $N_{Si} \leq 4$ has already been accounted for, the concentration of **7** in relation to these other oligomers strongly implies that it consists of 5 or 6 Si atoms. The correlations of the −97.76 ppm peak with resonances at −88.81 and −90.85 ppm furthermore indicate that **7** contains a silicon network of the form $Q^2-Q^3-Q^{3t}$. If we add the constraint that only 2 or 3 silicon atoms can be added to this unit to complete the structure, then the most plausible explanation is that **7** is a stereoisomer of the tricyclic hexamer I. The 1- and 2-D correlation spectra of **7** are similar to those of the tricyclic hexamer I, and we have confirmed that the major features of the experimental COSY spectrum (Figs. 3a and 4) can indeed be replicated by simulations that assume **7** is a stereisomer of tricyclic hexamer I.

The tricyclic hexamer I potentially has four chiral Si atoms depending on the orientations of the OH groups and the different acid sites, and thus could have multiple diastereomers in addition to possible conformers. We have analyzed the neutral (i.e., all nonbridging oxygens protonated), unsolvated tricyclic hexamer I, and among the potential stereoisomers only a single energy minimum was identified. Inversion at one of the Q^3 or Q^{3t} sites of this structure to form other diastereomers was invariably found to point the inverted center's nonbridging oxygen in energetically unfavorable directions and destabilize the molecule. Our calculations have been done for the neutral oligomer. A tricyclic hexamer I anion with a stable structure that loses a proton from a different hydroxyl than observed for bicyclic hexamer I and suppressed proton exchange at the negatively charged site could give rise to the signals we have observed.

If we accept the assignment of **7** as a stereoisomer of the tricyclic hexamer I (or a stable anion), we observe that three of the eight nearest neighbor scalar interactions in this oligomer can be categorized as strong or intermediate couplings. The dependence of the cross-peak splittings and patterns on these *J* values is strongly nonlinear, and refinement of the *J* values is a complicated task. The Q^2-Q^{3t}(A) coupling is especially problematic. The cross-peaks of this correlation almost completely overlap the stronger Q^2(A)−Q^2(B) cross-peaks of the monosubstituted cyclic tetramer, and the active coupling cannot be accurately determined. Since the cross-peaks even of remote spins are affected by the strong couplings, there are relatively large uncertainties in all of the *J* values of this oligomer. All of the putative *J* values nevertheless lie within ranges established by previous studies for the associated Q^x-Q^y interaction.[15]

Oligomers 8 and 9. The chemical shifts of the oligomer **8** resonances suggest a structure consisting of two distinct Q^2 sites and one Q^3 site. The cross-peak pattern of the (−88.41, −97.31) correlation indicates that the −88.41 ppm multiplet to first order is a triplet, with a splitting of 6.5 Hz (Figs. 3a). Since the −97.31 ppm resonance is also correlated with the −89.66 ppm resonance, it may be inferred that the oligomer contains units

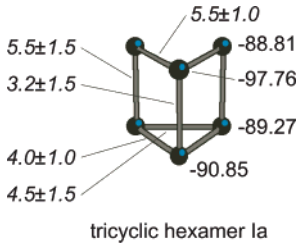

Figure 12. Proposed silicon network of oligomer **7** with the *J* and chemical shift parameters of the simulation that was the best match to the experimental COSY spectrum. The network has the same internuclear connectivities as the tricyclic hexamer I, and is assumed to be a stereoisomer.

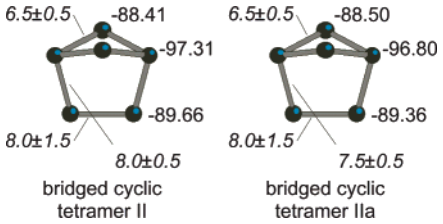

Figure 13. Proposed silicon networks of oligomers **8** (*left*) and **9** (*right*) with the *J* and chemical shift parameters of the simulations that were the best matches to the experimental COSY spectrum. The structures are stereoisomers of each other.

of the form $-Q^2(A)-Q^3-Q^2(B)-Q^3-Q^2(A)-$, with the $Q^2(B)$ site corresponding to the -88.41 ppm resonance. The $Q^2(A)$ resonance exhibits no other correlations, so we conclude that it is connected to another $Q^2(A)$ site or to a Q^3 site. In addition, the intensities of the three peaks are in a range comparable to the intensities of oligomers with 5 and 6 Si atoms.

Figure 13 displays an oligomer that is consistent with these findings. Simulated cross-peak patterns that agree well with the experimentally observed ones are obtained with the parameters shown in this figure. However, it is also possible to explain these results and obtain simulations that match experimental spectra by assigning **8** to the bridged cyclic tetramer (Figure 1). Although it is usually assumed that the Q^2 sites of this oligomer are magnetically equivalent, we have identified energy minima corresponding to structures in which the symmetry is removed. If the sites do not interconvert rapidly on the time scale of the measurement, the NMR signals of the Q^2 sites will appear as separated lines.

The oligomer **9** 2-D correlation spectrum resembles that of oligomer **8**, both in the chemical shifts of correlated resonances and in the cross-peak patterns. The same reasoning that led to the deduction of the structure of oligomer **8** therefore applies to **9**. Because the bridged cyclic tetramer II structure contains two potential chiral centers, diastereomers as well as conformers are a topological possibility, and simulations that correspond closely to the experimental spectra can be obtained by assuming **9** is a diastereomer of **8** (Figure 13). However, as for the tricyclic hexamer I, geometry optimization of the unsolvated, neutral oligomer reveals the existence of only one stable stereoisomer, and solvation or charge effects may need to be invoked to identify other stable structures of this oligomer just as for **7**.

Isomerism and Relative Energies of Other Oligomers. Harris and Knight found experimental evidence for two diastereomers of the oligomer they called the tricyclic hexamer II,[15,26] even though five diastereomers can be constructed with this network (Figure 14). We have determined that energy minima exist for all five diastereomers, but three of the energies

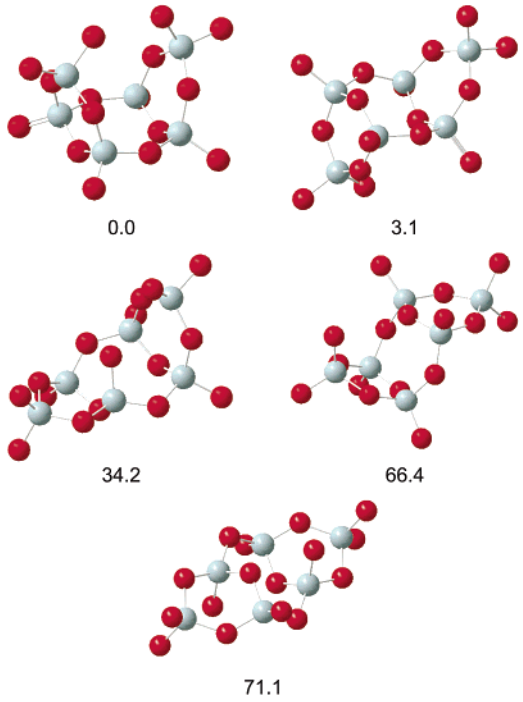

Figure 14. Energy-minimized structures of the tricyclic hexamer II diastereomers, with total energies in kcal/mol.

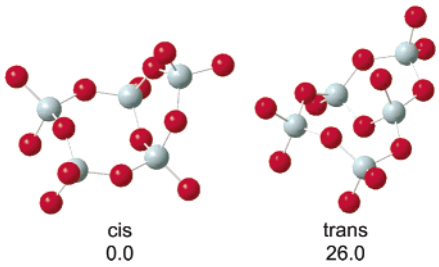

Figure 15. Energy-minimized structures of the bicyclic pentamer's diastereomers, with total energies in kcal/mol.

are 31.1 kcal/mol or higher than the lowest two, which are separated by only 3.1 kcal/mol. Thus, if the diastereomer populations are thermally equilibrated at room temperature, the oligomer's total population would be dominated by the two lowest-lying diastereomers, as is observed experimentally.

A similar argument can explain other instances of undetected diastereomers. As one example, we consider the bicyclic pentamer, which in principle can have two diastereomers (Figure 15). Our calculations show that energy minima can be found for both diastereomers, but the separation in energy is so large that the population of the *trans* form will be an undetectable fraction of the *cis* isomer.

Energy calculations of oligomers that are not necessarily stereoisomers also results in interesting comparisons. The tricyclic hexamer I is the most stable six-silicon molecule followed by the tricyclic hexamer IIA and IIB, which are 2.5 and 5.7 kcal/mol higher in energy, respectively. The doubly bridged cyclic tetramer is 3.3 kcal/mol higher in energy. The observation of the higher energy species in solution can have two explanations. The first is that silicate species formation is being controlled kinetically. The second is that the energies of the different structures are more nearly equal when solvation and ionic states (loss of protons) are taken into consideration. Similarly, for the bicyclic hexamers, the bridged cyclic tetramer

Table 4: Calculated ^{29}Si Chemical Shifts (ppm from DSS) and Their Deviations from Experimentally Determined Values $\delta_{exp} - \delta_{calc}$ (in parentheses)

Oligomer	Q^1	Q^2		Q^{2t}	Q^{3t}	Q^3
		chain	ring[a]			
dimer	−78.5 (−3.0)					
linear trimer	−80.6 (−0.5)	−88.0 (−1.7)				
cyclic trimer				−85.9 (3.0)		
linear tetramer	−79.1 (−2.0)	−86.3 (−3.0)				
cyclic tetramer			−89.4 (0.4)			
monosubstituted cyclic trimer	−77.5 (−3.5)			−84.7 (2.1)	−88.9 (−2.1)	
monosubstituted cyclic tetramer	−77.0 (−3.8)		−88.4 (−0.4) (A)			−97.9 (0.8)
			−92.4 (3.2) (B)			
bicyclic pentamer			−88.4 (−1.0)	−84.1 (1.5)	−91.7 (1.8)	
bridged cyclic tetramer			−89.7 (2.7)			−99.6 (4.9)
prismatic hexamer					−93.2 (3.3)	
tricyclic hexamer I			−93.1 (4.1)		−93.7 (3.4) (A)	−99.8 (2.2)
					−91.7 (2.4) (B)	
tricyclic hexamer IIa (*cisoid*)				−86.3 (3.1)	−95.3 (5.9)	
tricyclic hexamer IIb (*transoid*)				−84.4 (1.0)	−87.9 (−2.7)	
doubly bridged cyclic tetramer			−90.9 (3.6)			−99.3 (5.2)
pentacyclic heptamer			−90.3 (−0.1)		−89.1 (−2.8)	
					−89.1 (−1.6)	
cubic octamer						−105.2 (7.0)
hexacyclic octamer					−98 (4.8) (A)	−105.3 (5.8)
					−95.1 (4.5) (B)	
trisubstituted monomer	−79.6 (−1.1)					−99.5 (1.9)
bicyclic tetramer				−82.1 (0.9)	−84.6 (−6.3)	
linear pentamer	−80.0 (−1.2)	−88.6 (−0.6)				
		−86.6 (−2.8)				
bicyclic hexamer I				−85.4 (2.7)	−97.4 (6.5)	
bicyclic hexamer II			−91.7 (2.4)			−101.4 (3.6)
bicyclic hexamer IIa			−88.2 (−1.0)			−92.7 (−4.3)
bridged cyclic tetramer IIa			−82.4 (−6.1)			−94.4 (−2.4)
			−87.7 (−1.7)			
$\overline{\lvert\delta_{exp}-\delta_{calc}\rvert}$	2.1	2.0	2.2	2.0	3.7	3.8

[a] Excludes Q^2 atoms in three-silicon rings (next column).

II is the most stable species, followed by the *cis* and *trans* forms of the bicyclic hexamer II (0.3 and 6.6 kcal/mol higher, respectively) and the bicyclic hexamer I (9.8 kcal/mol higher). As other examples, the cyclic tetramer is 4.5 kcal/mol more stable as compared to the monosubstituted cyclic trimer, the cubic octamer is 8.2 kcal/mol more stable as compared to the hexacyclic octamer, and the bridged cyclic tetramer is 2.6 kcal/mol more stable as compared to the bicyclic pentamer. Thus if all of these structures are formed, kinetic control is the dominant effect.

Comparison of Experimental and Calculated ^{29}Si Chemical Shifts. Chemical shifts calculated by the GIAO method and averaged as described in the Computational section are listed in Table 4. Also presented in the bottom row of the Table is the average magnitude of the deviation of the calculated and measured shifts. This Table reveals that the difference between the measured and computed shifts is consistently larger for Q^{3t} sites and Q^3 sites as compared to other types of Q species. Furthermore, the calculated shifts for Q^1 and Q^2 chain sites are uniformly higher than the experimental values, whereas for Q^{2t} sites the theoretical results are skewed low, suggesting that there may be a systematic error in the way the shifts or local environments are determined for these sites.

It has been demonstrated both experimentally and theoretically that the ^{29}Si chemical shift in silicates is quite sensitive to the Si−O−Si bond angle and decreases with increasing angle.[51] This angle is also easy to vary as the bending potential is very low. A skewing of the calculated shifts for certain Q sites might therefore reflect the systematic effects of solvation and different ionization sites. The magnitude of the ionization effect alone is illustrated by the chemical shift behavior of the monomer, which we and others[47] have found to move in the positive direction by a few ppm when a proton is removed from the neutral monomer to form the −1 ion.

The actual geometries in solution could be different from optimized gas-phase structures due to different hydrogen bonding patterns and charge states. In particular, differences in the bond angles in the free molecule and the molecule in solution could explain most of the differences in the experimental and calculated chemical shifts. This is consistent with the dependence of the chemical shifts on the local DFT and B3LYP geometries as noted earlier.

Silicon-29 Homonuclear Scalar Couplings. Two-bond scalar couplings determined in ^{29}Si-enriched samples are compiled in Table 5. The *J* values of the new oligomers we have proposed in this Article are seen to lie within or near the ranges established by previous measurements.[15,26] For some Q^m-Q^n interacting pairs the *J* couplings are found to be characterized by narrow limits, while for other pairs the dispersion in *J* values is much larger among oligomers. As a group, the largest scalar couplings are those involving one Q^1 site, which are clustered between 6.6 and 8.0 Hz. The smallest interactions are those between Si atoms in the same three-Si ring, e.g., $Q^{2t}-Q^{3t}$, which lie from 3.3 to 4.5 Hz.

The implication of these observations is that the parameters governing *J* couplings have a narrower range of allowed values

(51) Engelhardt, G.; Radeglia, R. *Chem. Phys. Lett.* **1984**, *108*, 271−274. Tossell, J. A.; Lazzeretti, P. *Phys. Chem. Minerals* **1988**, *15*, 564−569. Xue, X.; Kanzaki, M. *Phys. Chem. Minerals* **1998**, *26*, 14−30.

Table 5: Two-bond $^{29}Si-^{29}Si$ Scalar Couplings (Hz) in Silicates: Dependence on Interacting Q Species

Oligomer	Q^1–Q^2	Q^1–Q^3	Q^1–Q^{3t}	Q^2–Q^2	Q^2–Q^3	Q^2–Q^{3t}	Q^{2t}–Q^{3t} [a]	Q^3–Q^3	Q^3–Q^{3t}	Q^{3t}–Q^{3t} [a]	Q^{3t}–Q^{3t} [b]
linear trimer[c]	6.9										
linear tetramer[c]	6.7			7.9							
monosubstituted cyclic trimer[c]			6.6				3.6				
monosubstituted cyclic tetramer[c]		6.8		6.5	6.5						
bicyclic pentamer[c]				8.0		5.4	3.8			3.4	
bridged cyclic tetramer[c]					5.4						
tricyclic hexamer I[c]					7.6	5.6			4.8	3.3, 4.4	
tricyclic hexamer IIa (*cisoid*)[c]							3.9			3.3	5.7
tricyclic hexamer IIb (*transoid*)[c]							3.9			3.3	5.7
doubly bridged cyclic tetramer[c]					5.6			4.4			
pentacyclic heptamer[c]						7.5				4.3, 3.3	5.7
hexacyclic octamer[c]								5.0	5.8	4.3, 3.3	9.8
trisubstituted monomer		7.5									
bicyclic tetramer							4.2				
linear pentamer	8.0			7.5							
bicyclic hexamer I							4.5				3.0
bicyclic hexamer II				5.0	7.0			4.5			
bicyclic hexamer IIa				5.0	6.5			4.0			
tricyclic hexamer Ia					5.5	5.5			3.2	4.0, 4.5	
bridged cyclic tetramer II				8.0	8.0, 6.5						
bridged cyclic tetramer IIa				8.0	7.5, 6.5						
Mean	**7.2**	**7.2**	**6.6**	**7.0**	**6.6**	**6.0**	**4.0**	**4.5**	**4.6**	**3.8**	**6.0**
Standard deviation	**0.7**	**0.5**		**1.3**	**0.9**	**1.0**	**0.3**	**0.4**	**1.3**	**0.5**	**2.4**

[a] Coupled nuclei are in the same three-Si ring. [b] Coupled nuclei are in different three-Si rings. [c] Data from Harris and Knight.[15,26]

in some structural units than in others. In some cases, the narrow limits are associated with an inflexible, closed structure that permits little variation in bond angles and lengths. The narrow *J* ranges for Q^1 sites can be attributed to the absence of networks, i.e., oxygen bridges to two or three Si neighbors, that can force the local bonding into a variety of extreme geometries.

Table 5 also shows a correlation between local structure and the magnitude of the *J* coupling, wherein Si−O−Si units that are able to relax into favorable "ideal" geometries have *J* couplings that are approximately twice as large as those of Si−O−Si units in more strained configurations. Examples of the former include Si pairs involving one Q^1 site, and Q^2-Q^2 or Q^2-Q^3 linkages in either a linear arrangement or four-Si ring, whereas the latter group consists mainly of Si−O−Si units in a three-Si ring. The ^{29}Si-^{29}Si two-bond *J* coupling, like the ^{29}Si chemical shift, can thus be regarded as a sensitive empirical measure of local structure in silicate networks. Several studies have confirmed the strong dependence of an electronic property on the Si−O−Si bond angle, viz., the ^{29}Si chemical shift, [51] but to our knowledge a theoretical analysis at a comparable level on the two-bond scalar interaction has not been undertaken.

5. Conclusion

Prior work on the determination of solution state structures of silicate oligomers has depended on 1-D ^{29}Si NMR methods that are practical and effective for oligomers with well-resolved, minimally overlapped spectra. The shortcomings of this approach are reflected in the numerous resonances that could not be assigned in the past, which are mainly located in chemical shift ranges where spectral overlap is severe, such as the −91 to −88 ppm and −98 to −96 ppm regions. The improved dispersion of the 2-D spectra reported here reveals several multiplets and internuclear correlations that were hidden in 1-D experiments. The 2-D cross-peak patterns provide additional detailed insights, and have enabled us to identify several new small oligomer structures.

A notable finding of the correlation experiments is that the newly detected oligomers contain only a small number of chemically inequivalent silicon sites, in most cases three or less. In addition, from the integrated 1-D peak intensities it can be inferred that the new oligomers are comparable in concentration to the small oligomers discovered in the past. These observations imply that the new oligomers should have relatively simple, small, symmetric structures. From a survey of traditional ball-and-stick drawings of oligomer structures, it might appear that there are too few plausible candidate structures with $N_{Si} \leq 6$ to support this conclusion, but such drawings fail to adequately represent the multiplicity of isomeric forms a silicate network can assume, especially when the potential chirality of Q^3 and Q^{3t} sites is considered. Computational models confirm that several oligomers have several stereoisomers that are stable energy minima, and thus are satisfactory structures.

The chirality of certain silicon sites greatly expands the spectrum of geometries that a silicate network can have, both in solution state species and in solid lattices. These diastereomers will have different NMR parameters, chemical properties, and structures, which suggests greater attention will be needed in future experimental and theoretical studies in the specification of silicate structures with the potential for configurational and conformational isomerism.

Acknowledgment. This research was supported by the U.S. Department of Energy's Environmental Management Science Program under the project entitled "The Aqueous Complexation Reactions of Anionic Silica and Uranium Species", Project Number 30944. The Pacific Northwest National Laboratory is operated for the U.S. Department of Energy by the Battelle Memorial Institute under contract no. DE-AC05-76RL01830.

Supporting Information Available: Author list for ref 46; atomic coordinates, total energies (a.u.), and zero point energies (kcal/mol) of DSS and silicate oligomers; relative energies (kcal/mol) of silicate oligomers; theoretical and experimental ^{29}Si chemical shifts (ppm from DSS) of silicate oligomers. This material is available free of charge via the Internet at http://pubs.acs.org.

JA0559202